Journal of Power Technologies 101 (1) (2021) 44–53

Applicability of Polyimide Membranes for Air Separation in Oxy-MILD Power Plants: Semi-Experimental Research

Leszek Remiorz[1], Grzegorz Wiciak[1], SettingsKrzysztof Grzywnowicz[1,✉], and Katarzyna Janusz-Szymańska[1]

[1]Politechnika Śląska / Silesian University of Technology

Abstract

The paper presents the results of experimental and computational research concerning the parameters of the separation process of N_2/O_2 mixture, regarding the composition of ambient air, using capillary polyimide membranes. The analysis focused on the potential applicability of polyimide membranes in oxy-MILD combustion units. The experimental data, collected using a sophisticated experimental test stand, was used to approximate continuous functions, describing the dependencies of essential parameters of the air separation process on variable operational conditions. These functions were used as fundamental blocks to develop a complete mathematical model of the membrane separation unit (MSU), including polyimide membranes and additional equipment, intended for use within oxy-MILD power generation units. Computational research was performed for three variants of MSU unit configuration, including: serial connection of membrane modules, multiple retentate recirculation and multiple permeate recirculation. Results, presented in the form of characteristic curves of investigated dependencies, indicate that the highest parameters of the separation process were gained for serial connection, whereas the lowest were for permeate recirculation. The collected data suggests that retentate recirculation might be beneficial for specific conditions, with limited application for continuous operation.

Keywords: ambient air separation, membrane separation, polyimide membranes, membrane separator design, oxy-MILD combustion

1 Introduction

The techniques of energy and heat production, due to their crucial influence on local and global markets, have for years remained the subject of wide and profound scientific research [1]; [2]; [3]; [4]; [5], both experimental and theoretical [1]; [6]; [7]. Worldwide electrical energy demand is rising continuously, driven by rapid economic development in numerous regions. Furthermore, since technological processes of energy generation are mainly based on the combustion of fossil fuels, this gives rise to higher consumption of primary energy sources, such as coal, natural gas, and crude oil, influencing emissions of greenhouse gases. Among these gases, carbon dioxide and water vapor as the ones most responsible for the greenhouse effect, should be mentioned [8]; [9]; [10]. Due to their negative impact on humans and the natural environment, a range of compounds coming from combustion of fossil fuels should be separated from the stream of exhaust gases before they are released to the atmosphere [1]; [11]. Similarly, compounds affecting global warming should be separated too [1]; [8]; [12]; [13].

Considering the reduction of CO_2 emissions, modern power generation units utilize various technologies, such as carbon capture and storage (CCS) installations [2]; [11]. In order to introduce such installations, three technological concepts are used: pre-combustion – capturing CO_2 before burning the fuel, post-combustion – capturing CO_2 after burning, and oxy-combustion – burning fuel under high oxygen concentration conditions [14]; [15]; [16] .

The main goal of oxy-combustion is to increase the percentage share of CO_2 in the total stream of exhaust gases leaving the combustion chamber [16]. The oxygen stream, used as the oxidizer instead of air, is produced in an air separation unit, where ambient air is separated into streams of oxygen and nitrogen with residual traces of other gases. The use of pure oxygen could trigger serious engineering and operating challenges [3]. Innovative Moderate or Intense Low Oxygen Dilution (MILD) technology increases the efficiency of the power generation unit while reducing emissions of target pollutants such as NO_x and CO [17]; [18]. Oxy-MILD combustion technology, which combines the advantages of both oxy-combustion and MILD technologies, uses a concentration of oxygen in the oxidizer stream of no more than 40%, to prevent a significant drop in the content of heat absorbing compounds, such as N_2 and CO_2, within the primary stream of exhaust gases. The main effect of insufficient N_2 and CO_2 is a substantial rise in

Table 1: Comparison of characteristic features of the gas separation technologies

	PSA	TSA	Membrane
Commercial maturity	mature	developing	developing
Availability of medium- or large-power systems	available	available with limitations	limited
Expected quality of the process	high	moderate to high	moderate to high
Complexity of the control systems	moderate	moderate to high	low to moderate
Expected investment costs for industrial-scale units	moderate	moderate to high	high
Expected maintenance costs for industrial-scale units	moderate to high	moderate to high	low to moderate

the temperature of the exhaust gases [17], promoting excessive generation of thermal NO_x among others. The separation of oxygen from ambient air might be performed by different techniques, including pressure swing adsorption (PSA), temperature swing adsorption (TSA) and membrane units. The most common of them are briefly characterized in Table 1 [18]; [19]; [20]; [21]; [22].

Utilization of membrane methods, based on semipermeable films (membranes) made from polymeric and other materials [23]; [24]; [25], might introduce major benefits compared to commonly implemented, commercially mature technology of pressure swing adsorption (PSA). The benefits come primarily from the internal construction of the membrane modules, lacking permanent adsorbents, and requirement for alternating depressurization of the adsorber vessel.

The membrane separation module (membrane separator) consists of a set of single membrane modules, connected either in parallel or series. More sophisticated combinations of these simple connections are often applied. Complete modules are compact in size, which is a crucial feature favoring widespread introduction of carbon capture installations in existing power generation units and other industrial plants with high CO_2 emissions [26]; [27]. The consideration of type, sizing and characteristics of the membrane modules, which are fundamental to the construction of a membrane separator, depends primarily on the budget and the desired nominal operational parameters of the separation unit [2]; [12]; [28]. Thus, optimizing the configuration of a membrane separation unit, regarding its internal construction, is a key task.

This paper presents a semi-experimental analysis of the operational parameters of selected variants of the membrane separator configuration. A semi-empirical model was constructed on the basis of the experiment to predict the variability of complex parameters of the separator [18].

2 Theory

2.1 Experimental Research

The experimental test stand utilized during the fundamental, experimental part of the research is presented schematically in Fig. 1 [18].

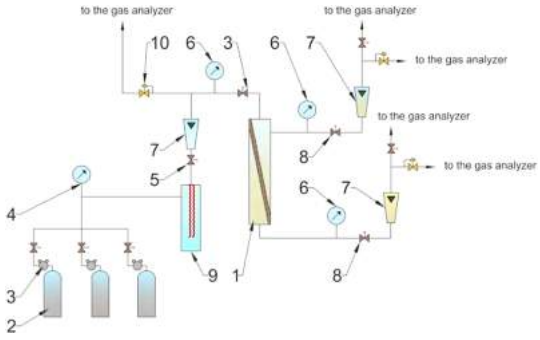

Figure 1: Chart of the experimental test stand: 1 - membrane module, 2 - external tanks of gaseous mixture, 3 - pressure reducers, 4 - pressure and temperature measurement, 5 - throttling valve, 6 - gauge manometer, 7 - flow measurement, 8 –pressure control throttling valves, 9 – the temperature and humidity control unit, 10 – safety evacuating valve [18]

During the experimental analysis, the module (Fig. 1, point 1) was fed with an artificial mixture of gases at initial temperature of 15°C, stored in external tanks (Fig. 1, point 2) of 10m3 total volume under a pressure of 200 bar. As safety and control equipment, multiple two-stage pressure reducers were used to reduce and stabilize the pressure of the feed (Fig. 1, point 3). The setup was equipped with a feed temperature and humidity control unit (Fig. 1, point 9) including an electric heater, to maintain the temperature of the inflowing mixture at 23°C.

The selected artificial feed simulated dry air and

consisted exclusively of nitrogen (79%) and oxygen (21%). At the outflow duct of the pressurized vessel, a set of measuring instruments (Fig. 1, point 4), including a gauge manometer and a thermocouple, were located. An additional throttling valve (Fig. 1, point 5) at the same duct acted as an additional flow stabilizer. The gaseous mixture was supplied to the membrane module, consisting of an NM-B02A capillary membrane (55 mm diameter and 360 mm length; 400 l/h flow at nominal conditions) produced by UBE Industries Ltd., Japan. The membrane was selected based on its worldwide commercial availability and relatively low market price (compared to rival products) – a key factor affecting investment cost in large-scale membrane separation units [23]; [27]; [29]. The final measurement and control units were located at the outlet ducts of the separation unit and contained pressure sensors (Fig. 1, point 6), thermocouples, and flow measurements instruments in the form of rotameters (Fig. 1, point 7). The control function of the unit was fulfilled by additional throttling valves (Fig. 1, point 8), responsible for regulating the flow of the permeate and retentate streams transported to the gas composition analyzers [18].

Two customized oxygen/carbon oxides gas analyzers (Servomex® 4900 and AtestGaz® PI-044) were used.

During the experimental part of the research, a number of key separation process parameters were investigated. The literature [4]; [9]; [17]; [23] identified these parameters as:

1. purity of the permeate, meaning the concentration of oxygen in the permeate stream, YO_2,
2. recovery coefficient R, meaning the ratio of elementary oxygen flows in the permeate and feed streams, defined by Eq. 1,
3. real separation factor α, meaning ratio of the concentrations of the ingredients of the mixture in the permeate stream relative to the ratio of the concentrations of the ingredients in the retentate stream, defined for oxygen with respect to nitrogen, as given by Eq. 2.

$$R = \frac{n_P YO_2}{n_f XO_{2f}} \tag{1}$$

where: n_p - molar stream flow of permeate, YO_2 - oxygen content in the permeate, n_f - molar stream flow of feed, XO_{2f} - oxygen content in the feed

$$\alpha = \frac{\left(\frac{YO_2}{XN_2}\right)}{\left(\frac{XO_{2r}}{XN_{2r}}\right)} \tag{2}$$

where: XN_2 - nitrogen content in the permeate, XO_{2r} - oxygen content in the retentate, XN_{2r} - nitrogen content in the retentate.

These values were obtained on the basis of direct measurements on the feed, permeate, and retentate streams, respectively. These measurements were performed by respective instrument, located in appropriate ducts, as well as the gas composition analyzers [18], under unsteady flow conditions (with feed flow regulated in the range 500-950 l/h, retentate flow in the range 100-500 l/h and permeate flow in the range 20-350 l/h) and variable retentate pressure (up to 6 bar) [18].

Values of subsequent investigated parameters were collected together with the operational conditions of the membrane unit. Sets of respective data were then analyzed in order to perform the curve fitting process. The fitting of a continuous function curve was performed using the least squares method. The best fits were selected on the basis of the highest values of the Pearson product-moment correlation coefficients for the respective sets.

2.2 Computational Analysis

The experimental research delivered the data on which a set of empirical functions was obtained that described the dependence of key parameters of the separation process quality on the environmental conditions. The continuous mathematical functions, obtained for a single membrane module on the basis of a curve fitting process, were then used as fundamental functions of the mathematical model of the separation unit. To ensure the accuracy of computational results, the model of a separation unit was extended to include a description of the Joule-Thomson effect, which appears in real units [30].

The computational algorithm included within the mathematical model of the unit is presented in chart form in Fig. 2.

The set of empirical dependencies shown on the algorithm chart (Fig. 2), included a list of polynomial functions of either fourth or second order, indicated in the form of Eq. 3-9.

The functions showing the dependence of the real separation factor on permeate (Q_p) and feed (Q_f) stream flows, introduced by Eq. 3 and Eq. 4, respectively, were obtained on the basis of a least squares method approximation for six points referring to the results of the experiment.

$$\alpha = 7e^{-5}{Q_p}^2 - 122.4e^{-3}Q_p + 52.3 \tag{3}$$

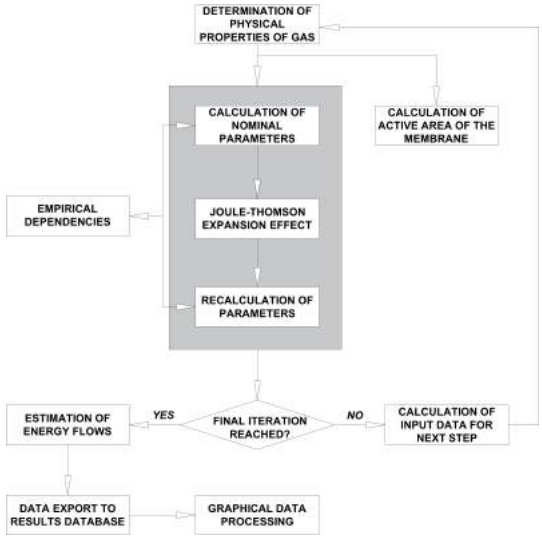

Figure 2: Algorithm of calculations and computational data processing [18]

$$\alpha = 7e^{-7}{Q_f}^2 - 5e^{-4}Q_f + 1 \tag{4}$$

Functions describing the oxygen recovery coefficient (R) in the permeate with respect to the permeate (Q_p) and the feed stream flows (Q_f), presented in the form of Eq. 5 and Eq. 6, respectively. As with the previous equations, these functions were estimated on the basis of: six measurements in the equation showing the dependence of (R) on the permeate (Q_p) and 18 points in the equation showing the dependence of (R) on the feed (Q_f).

$$R = 9e^{-4}{Q_p}^2 - 1.4551Q_p + 624.4 \tag{5}$$

$$R = -5e^{-11}Q_f^4 + 2e^{-7}Q_f^3 + 2e^{-4}Q_f^2$$

$$+66.9e^{-3}Q_f + 20 \tag{6}$$

Dependencies Eq. 7 and Eq. 8, indicating permeate purity (YO_2) with respect to the permeate (Q_p) and feed (Q_f) stream flows, respectively, were based on values acquired for a series of 18 measurements. The final model included all of the presented equations concerning the functions stated for the permeate and the feed flows. The double statement of the respective values (separation factor, recovery coefficient and permeate purity) was a crucial element for the purpose of obtaining high accuracy for the calculations, as both the permeate and retentate in any module might be used as the feed for another module in the computational model. Furthermore, their results might be compared, depending on the configuration of the modelled unit.

$$YO_2 = -1e^{-3}{Q_p}^2 + 1.6795Q_p + 631.3 \tag{7}$$

$$YO_2 = 9e^{-11}{Q_f}^4 - 3e^{-3}{Q_f}^3 + 4e^{-4}{Q_f}^2$$

$$+162.4e^{-3}Q_f + 100 \tag{8}$$

Due to the limited utilization of the function presented in Eq. 9, caused by a required decrease in the computational cost of the analyses, this function was not doubled in the model by any other equation describing oxygen concentration in the retentate.

$$XO_{2r} = 3e^{-6}{Q_f}^2 - 3.2e^{-4}Q_f \tag{9}$$

3 Results

3.1 Results of the Experimental Research

Fig. 3a and Fig. 3b depict the characteristic curves of the oxygen recovery coefficient (R) and the permeate purity (YO_2), obtained for constant retentate stream (Q_r) equaling Q_r = 500l/h, at varying feed pressure [18]. Fig. 4a and Fig. 4b show the results of the permeate purity (YO_2) and the oxygen recovery coefficient (R) versus the retentate stream flow (Q_r), at constant pressure equal to 5/6 bar, respectively. Fig. 4c and Fig. 4f show data from the NM-B02A membrane module, regarding the dependence of variable permeate (Q_p) and feed flows (Q_f), as well as retentate pressure (p_R), on the real separation factor (α), permeate purity (YO_2) and the oxygen recovery coefficient (R) [18].

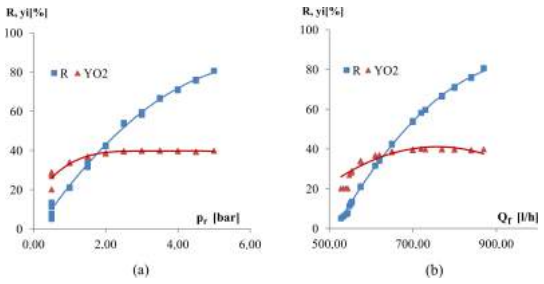

Figure 3: Characteristic curves for: (a) permeate YO_2 and R with respect to retentate pressure p_r, (b) permeate YO_2 and R with respect to feed flow Q_f

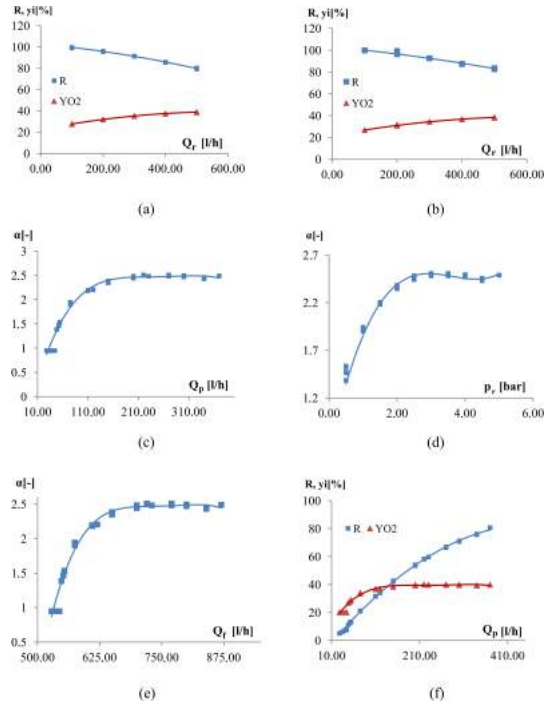

Figure 4: Experimental characteristic curves: (a) for the permeate YO_2 and R as a function of retentate flow Q_r for a pressure of 5 bar, (b) for the permeate YO_2 and R as a function of retentate flow Q_r for a pressure of 6 bar, (c) for α with respect to permeate flow Q_p, (d) for the real separation factor α with respect to retentate pressure p_R, (e) for α with respect to feed flow Q_f, (f) for the permeate YO_2 and R with respect to the permeate flow Q_p

3.2 Results of the Computational Research

The first of the analyzed configurations of the membrane separation units involved the serial connection of the membrane modules by the permeate duct. The principle of operation of the discussed configuration is based on the fact that the stream flow of the permeate from one module becomes the feed for the following one. The configuration of the discussed MSU, (system I) is schematically presented in Fig. 5.

Fig. 6a and Fig. 6b present the results of the computational analysis concerning the serial connection of modules. Figure 6a depicts dependence of the separation factor on a number of modules, for variable feed flow Q_f. The results of further investigation, shown in Fig. 6b, indicate the influence of the number of modules connected in series on permeate purity YO_2. The results of the investigation, presented in Fig. 6c, depict dependence of the minimum number of modules required to maintain permeate purity YO_2 exceeding 95%, under variable feed flow Q_f. Fig. 8a

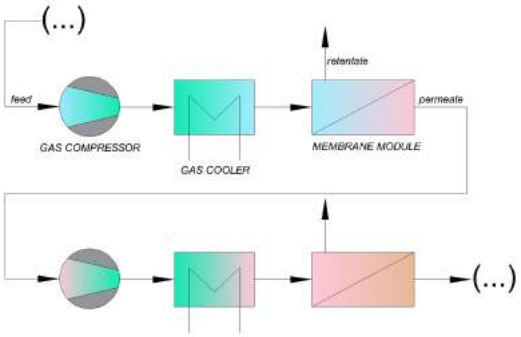

Figure 5: Chart of the membrane separator with serial connection of modules (system I) [18]

and Fig. 8b show the results concerning the second of the investigated separator configurations (system II), based on a single-membrane-module with multiple retentate recirculation. Fig. 7. schematically presents the discussed system, with essential elements connected. Figure 8a presents the dependence of oxygen concentration XO_{2r} in the retentate versus number of retentate recirculation stages n_C and primary feed flow values Q_f. The dependence of permeate purity on the number of stages of retentate recirculation for varying feed flows Q_f is depicted in Fig. 8b. The characteristic curve shown in Fig. 8c presents the residual content of oxygen in the retentate (for single-membrane separator) as a function of feed flow Q_f.

The last of the analyzed MSU configuration systems was the single-module separator with multiple permeate recirculation n_{CP}. Fig. 9 shows the investigated configuration. The resulting data, indicated in Fig. 10, present permeate purity YO_2 as a function of the number of permeate recirculation stages.

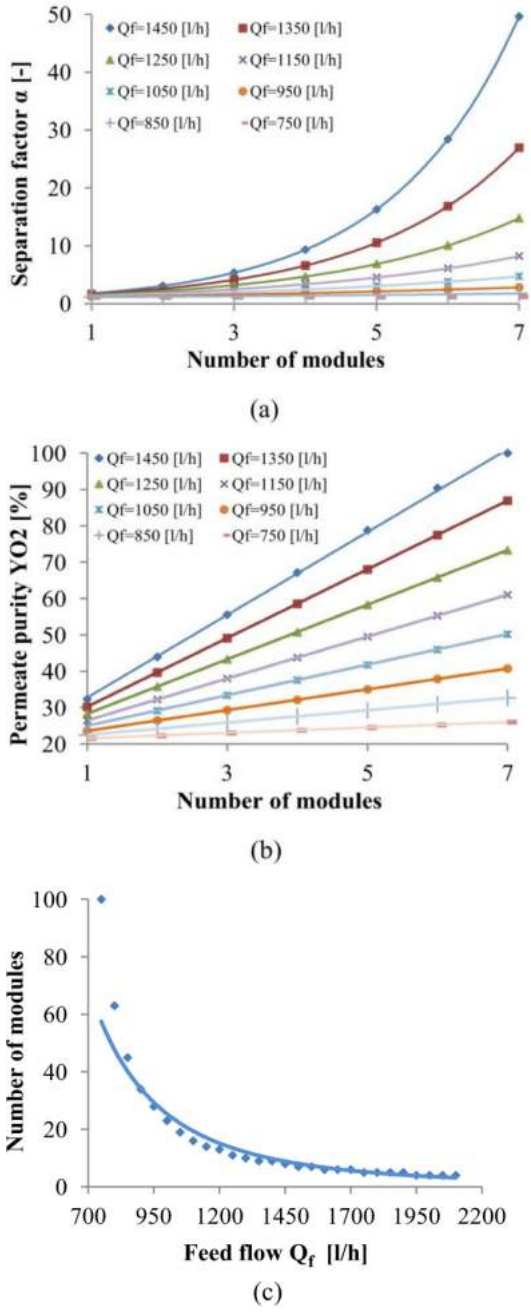

Figure 6: Characteristic curves of the variant with serial connection of modules: (a) separation factor as function of number of modules in series for varying feeds, (b) purity of the permeate vs. number of modules in series for varying feeds, (c) minimum number of modules in series required for $YO_2 > 95\%$.

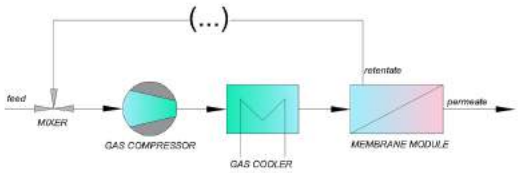

Figure 7: Chart of the separator with multiple recirculation of the retentate (system II) [18]

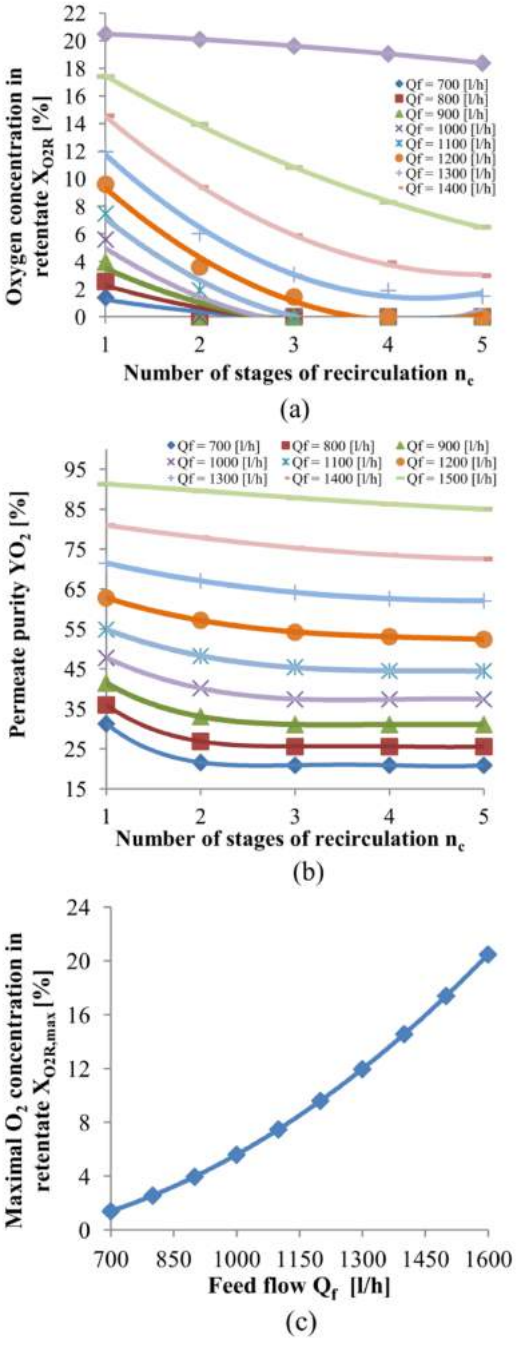

Figure 8: Characteristic curves of the variant with multiple retentate recirculation: (a) oxygen concentration in the stream flow as function of retentate recirculation stages for variable feed flows, (b) permeate purity as function of retentate recirculation stages for variable feed flows, (c) maximum oxygen concentration in the retentate as function of variable feed flow.

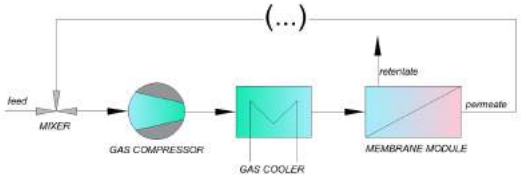

Figure 9: Chart of the separator with multiple recirculation of the permeate (system III) [18]

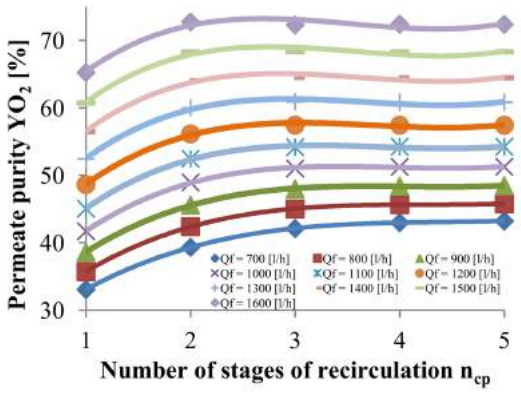

Figure 10: Dependence of permeate purity on number of recirculation stages for variable feed flows

4 Discussion

The results of the experimental research, acquired at constant retentate stream flow Q_r equal to 500 l/h, indicate that an increase in pressure of the retentate is followed by a rise of recovery coefficient R and permeate purity YO_2, as seen in Fig. 3a.

As depicted in Fig. 4c, at constant retentate stream flow value Q_r equal to 500l/h a rapid increase in separation factor α follows a rise in permeate flow Q_p. The key part of the acquired data concerns the results of the computational analysis. With reference to the serial connection-based MSU (system I), an increase in the number of modules in serial connection (Fig. 5) was followed by an exponential rise in the real separation factor α of the system, as shown in Fig. 6a. Nevertheless, the rate of change of separation factor α depends on the feed flow Q_f supplying the system. As indicated, for feed flows Q_f<1000 l/h, the value of separation factor α for a seven-module system corresponded to roughly twice the value of the separation factor for a single-module system. For feed flows exceeding $Q_f > 1200$ l/h, a seven-module unit is characterized with a rise of over 10 times in the separation factor. As regards permeate purity YO_2, an almost linear rise with the increase in the number of modules was observed for this configuration of the separator, as presented in Fig. 6b, with the peak value being 99%. However, the slope of the acquired trendline depends to a great extent on the feed flow – the highest values of oxygen concentration in the permeate were observed for the largest feed flow.

As shown in Fig. 8a, the MSU system concerning multiple retentate recirculation (system II, indicated in Fig. 7) might be used to reduce the oxygen concentration in the retentate. However, the results show strong dependence of the drop in oxygen concentration both on the number of recirculation stages n_C and feed flow Q_f. Regarding the feed flows $Q_f < 1000$ l/h, triple retentate recirculation is followed by the acquisition of retentate with almost no oxygen content. Nevertheless, further increase in feed flow Q_f results in a substantial rise in the number of recirculation stages required to obtain a similar effect. For the feed flows Qf > 1300 l/h, the oxygen fraction in the retentate takes significant values, independently on further rise in recirculation stages. For feed flows exceeding 1600 l/h, the maximum residual content of oxygen in the retentate might rise to 20%, as shown in Fig. 8c, which suggests an operating failure of the membrane. Furthermore, an increase in the number of retentate recirculation stages results in drop of the permeate purity, especially for low feed flows. As indicated in Fig. 8b, for feed stream flow of 700 l/h, introduction of double retentate recirculation is followed by a drop in permeate purity exceeding 10 percentage points.

As for the multiple permeate-recirculation configuration of the investigated separator (system III, shown in Fig. 9), the results of the computational analysis indicate a smooth rise in permeate purity YO_2 with an increase in the number of stages for lower feed flows ($Q_f < 900$ l/h). Nevertheless, significant fluctuations in purity are observed for feed flows exceeding 1300 l/h, with the peaks corresponding to either double or triple permeate recirculation.

5 Conclusions

Research concerning the membrane separator consisting of a number of modules connected in series showed an exponential increase in the real separation factor of the system with the increase in number of recirculation stages. However, the rate of rise of the factor clearly depends on the feed flow, with peaks observed for the highest flow rates. Therefore, one may conclude that the serial connection of modules in an industrial MSU unit might lead to major operational benefits in the case of large volumetric flows of the feed. Factoring in all the research results, including permeate purity, the serial connection of single modules seems to be the most beneficial in the case of the large flows of exhaust gases typically found at nominal operational states of industrial-scale power plants. Nevertheless, for the low and moderate feed flows occurring, for instance, during the start-up of the unit, the operational parameters of serial-connection MSU are insufficient for direct application in oxy-MILD technology.

Regarding the data obtained for the system based on multiple retentate recirculation, a substantial non-linear fall in oxygen concentration was observed in the permeate following a rise in the number of recirculation stages. The rate and value of the reduction in permeate purity depended on the feed flow value. Thus, the results clearly indicate that the introduction of retentate recirculation leads to a decrease in the operational parameters of the separation unit with regard to the purity of the permeate. This is caused by the significantly greater pressure losses between the feed and the permeate outlet than between the feed and retentate outlet in the membrane modules under consideration [18]. Multiple-retentate recirculation separators might be introduced for specific operational conditions of the plant, or where the retentate is an important by-product used in another part of the process, but the real applicability of such a configuration in most oxy-MILD power units is marginal.

Analysis of the results of MSU configuration with multiple permeate recirculation indicates a rise in permeate purity following an increase in number of permeate recirculation stages, especially with low feed flows (below 900 l/h). Nevertheless, for high feed flows, large fluctuations of the permeate purity, damping with a rise in the number of stages were observed during steady-status of the unit with further gas recirculation, which resulted in unstable performance and operation of the oxy-MILD unit. This might be explained by the oxygen transport capacity of the investigated membrane reaching the local limit.

As regards general application of investigated MSU configurations for their application as oxidizer sources in oxy-MILD power generation units, the research results indicate that the investigated membrane separation technology is only partially able to compete with mature methods. This basically corresponds to low to moderate purity of the permeate for simple construction of separators. In order to reach the goal, serial connection of multiple modules is required. This would necessitate a high number of compressors and potential substantial rise in overall power demand of the unit, which will be the subject of future investigation.

Acknowledgment

The research has been financially supported by the Silesian University of Technology by statutory research funds within the framework of project no.: 08/050/BK_21/0231.

References

1.Wiciak, G., and Kotowicz, J. (2011) Experimental stand for CO2 membrane separation. *Journal of Power Technologies*, **91**, 171–178.

2.Dryjańska, A., and Janusz-Szymańska, K. (2013) The analysis of economic efficiency of oxy-type power plant on supercritical parameters with a capacity of 600 MW. *Archivum Combustionis*, **33**, 109–123.

3.Davidson, J., and Thambimuthu, K. (2004) Technologies for capture of carbon dioxide. *Proceedings of the Seventh Greenhouse Gas Technology Conference*.

4.Remiorz, L., Rulik, S., and Dykas, S. (2013) Numerical modelling of CO2 separation process. *Archives of Thermodynamics*, **34**, 41–53.

5.Remiorz, L., Dykas, S., and Rulik, S. (2010) Numerical Modelling of Thermoacoustic Phenomenon as Contribution to Thermoacoustic Engine Model. *Task Quarterly*, **14**, 261–273.

6.Harasimowicz, M., Orluk, P., Zakrzewska-Trznadel, G., and Chmielewski, A.G. (2007) Application of polyimide membranes for biogas purification and enrichment. *Journal of Hazardous Materials*, **144**, 698–702.

7.Wiciak, G. (2012) Identyfikacja wybranych charakterystyk separacji CO2 membrany kapilarnej polimerowej. *Rynek Energii*, **100**, 94–100.

8.Fujimori, T., and Yamada, T. (2013) Realization of oxyfuel combustion for near zero emission power generation. *Proceedings of the Combustion Institute*, **34**, 2111–2130.

9.Yamauchi, Y., and Akiyama, K. (2013) Innovative Zero-emission Coal Gasification Power Generation Project. *Energy Procedia*, **37**, 6579–6586.

10.Verkhivker, G., and Yantovski, E. (2001) Zero-emissions gas-fired cogeneration of power and hydrogen. *International Journal of Hydrogen Energy*, **26**, 1109–1113.

11.Chmielniak, T., and Łukowicz, H. (2010) Condensing power plant cycle - assessing possibilities of improving its efficiency. *Archives of Thermodynamics*, **31**, 105–113.

12.Meyer, J., Mastin, J., Bjørnebøle, T.-K., Ryberg, T., and Eldrup, N. (2010) Techno-economical study of the Zero Emission Gas power concept. *Energy Procedia*, **4**, 1949–1956.

13.Sahand, S., Mahmoudi, S.M.S., Nami, H., and Yari, M. (2016) Energy and exergy analyses of a novel near zero emission plant: Combination of MATIANT cycle with gasification unit. *Applied Thermal Engineering*, **108**, 893–904.

14.Li, L., Duan, L., Tong, S., and Anthony, E.J. (2019) Combustion characteristics of lignite char in a fluidized bed under O2/N2, O2/CO2 and O2/H2O atmospheres. *Fuel Processing Technology*, **186**, 8–17.

15.Nami, H., Ranjbar, F., and Yari, M. (2018) Thermodynamic assessment of zero-emission power, hydrogen and methanol production using captured CO2 from S-Graz oxy-fuel cycle and renewable hydrogen. *Energy Conversion and Management*, **161**, 53–65.

16.Chen, W., Ham, L. van der, Nijmeijer, A., and Winnubst, L. (2015) Membrane-integrated oxy-fuel combustion of coal: Process design and simulation. *Journal of Membrane Science*, **492**, 461–470.

17.Perrone, D., Castiglione, T., Klimanek, A., Morrone, P., and Amelio, M. (2018) Numerical simulations on Oxy-MILD combustion of pulverized coal in an industrial boiler. *Fuel Processing Technology*, **181**, 361–374.

18.Remiorz, L., Wiciak, G., Grzywnowicz, K., and Janusz-Szymańska, K. (2019) Investigation of Applicability of Polyimide Membranes for Air Separation in Oxy-MILD Zero-Emission Power Plants. *Proceedings of the XIV Research and Development in Power Engineering Conference*, **137**, 01033.

19.Ben-Mansour, R., and Qasem, N.A.A. (2018) An efficient temperature swing adsorption (TSA) process for separating CO2 from CO2/N2 mixture using Mg-MOF-74. *Energy Conversion and Management*, **156**, 10–24.

20.Yang, M.-W., Chen, N.-chi, Huang, C.-hsiang, Shen, Y.-ting, Yang, H.-sung, and Chou, C.-tung (2014) Temperature swing adsorption process for CO2 capture using polyaniline solid sorbent. *Energy Procedia*, **63**, 2351–2358.

21.Zheng, L., Prossner, N.M., and Shah, M.M. (2011) *Oxy-Fuel Combustion for Power Generation and Carbon Dioxide (CO2) Capture*, Woodhead Publishing.

22.Bell, D.A., Towler, B.F., and Fan, M. (2010) *Coal Gasification and Its Applications*, Elsevier.

23.Lee, S., Yun, S., and Kim, J.-K. (2019) Development of novel sub-ambient membrane systems for energy-efficient post-combustion CO2 capture. *Applied Energy*, **238**, 1060–1073.

24.Rezakazemi, M., Sadrzadeh, M., and Matsuura, T. (2018) Thermally stable polymers for advanced high-performance gas separation membranes. *Progress in Energy and Combustion Science*, **66**, 1–41.

25.Scholes, C.A., Stevens, G.W., and Kentish, S.E. (2012) Membrane gas separation applications in natural gas processing. *Fuel*, **96**, 15–28.

26.Banaszkiewicz, T., Chorowski, M., and Gizicki, W. (2014) Comparative analysis of oxygen production for oxy-combustion application. *Energy Procedia*, **51**, 127–134.

27.Toftegaard, M.B., Brix, J., Jensen, P.A., Glarborg, P., and Jensen, A.D. (2010) Oxy-fuel combustion of solid fuels. *Progress in Energy and Combustion Science*, **36**, 581–625.

28.Zhang, D., Wang, H., Li, C., and Meng, H. (2017) Modelling of purge-gas recovery using membrane separation. *Chemical Engineering Research and Design*, **125**, 361–366.

29.Chen, W., Chen, C.-sheng, Bouwmeester, H.J.M., Nijmeijer, A., and Winnubst, L. (2014) Oxygen-selective membranes integrated with oxy-fuel combustion. *Journal of Membrane Science*, **463**, 166–172.

30.Bounaceur, R., Berger, E., Pfister, M., Andres, A., Santos, R., and Favre, E. (2017) Rigorous variable permeability modelling and process simulation for the design of polymeric membrane gas separation units: MEMSIC simulation tool. *Journal of Membrane Science*, **523**, 77–91.

31.Unger, N., Bond, T.C., Wang, J.S., Koch, D.M., Menon, S., Shindell, D.T., and Bauer, S. (2010) Attribution of climate forcing to economic sectors. *Proceedings of National Academy of Sciences of USA*, **107**, 3382–3387.